Qualitative Analysis and Quantitative Assessment of Changes in Neutral Glycerol Lipid Molecular Species Within Cells

REAGENTS

Cell culture

RAW 264.7 cells were obtained from American Type Culture Collection (Manassas, VA). Tissue culture reagents included high-glucose Dulbecco's Modified Eagle's Medium (DMEM) (Cellgro, Herndon, VA), fetal calf serum (Hyclone, Logan, UT), Dulbecco's Phosphate-Buffered Saline (D-PBS; Cellgro, Herndon, VA), and penicillin/streptomycin (Cellgro, Herndon, VA). The cells were carried in culture in either 150-cm^2 tissue culture flasks with filter caps or 100-mm^2 tissue culture dishes (Fisher Scientific, Fair Lawn, NJ).

Standards

All deuterium-labeled glyceryl lipids were [1,1,2,3,3]-d_5 in the glycerol backbone. The following lipids were obtained from Avanti Polar Lipids (Alabaster, AL): Kdo$_2$-lipid A; d_5-DAG mixture containing d_5-14:0/14:0 DAG, d_5-15:0/15:0 DAG, d_5-16:0/16:0 DAG, d_5-17:0/17:0 DAG, d_5-19:0/19:0 DAG, d_5-20:0/20:0 DAG, d_5-20:2/20:2 DAG, d_5-20:4/20:4 DAG, and d_5-20:5/20:5 DAG; d_5-TAG mixture containing d_5-14:0/16:1/14:0 TAG, d_5-15:0/18:1/15:0 TAG, d_5-16:0/18:0/16:0 TAG, d_5-17:0/17:1/17:0 TAG, d_5-19:0/12:0/19:0 TAG, d_5-20:0/20:1/20:0 TAG, d_5-20:2/18:3/20:2 TAG, d_5-20:4/18:2/20:4 TAG, and d_5-20:5/22:6/20:5 TAG.

Extraction and purification

High performance liquid chromatography (HPLC)–grade ammonium acetate(NH_4OAc), chloroform ($CHCl_3$), ethyl acetate, hexanes, isooctane, isopropanol, methanol, and methylene chloride (CH_2Cl_2) were obtained from Fisher Scientific (Fair Lawn, NJ). Optima-grade toluene and water also were obtained from Fisher Scientific (Fair Lawn, NJ). Discovery DSC-Si silica, and Discovery DSC-NH_2 amino propyl solid phase extraction cartridges, and the vacuum manifold were obtained from Supelco (Bellefonte, PA). Other equipment included a benchtop vortexer (Vortex Genie 2, VWR Scientific, West Chester, PA), Fluoropore 0.2-μm FG membrane filters (Millipore, Billerica, MA), 96-well polypropylene plates (Eppendorf, Westbury, NY), and Quant-iT DNA analysis kit (Molecular Probes, Eugene, OR).

METHODS
Cell culture

RAW 264.7 cells were grown in T-150 flasks containing 30 ml of complete growth medium consisting of 500 ml of high-glucose DMEM supplemented with 10% FBS and 1% penicillin/streptomycin. The cells were maintained in a humidified incubator at 37° with a 5% CO_2 atmosphere. They were split such that 2×10^6 cells were seeded in a new flask each time the cells reached 80% confluency. Briefly, when the cells reached this confluency (approximately every 2 to 3 days), the old growth medium was removed, and 10 ml of fresh medium, which had been previously warmed to 37°, was added. The cells were then scraped from the flask using a large disposable cell scraper. A 10-μl aliquot was counted using a haemocytometer. The volume of media determined to contain 2×10^6 cells was then added to a new T-150 flask, and the volume was adjusted to 30 ml with complete growth medium. The flasks were then placed back into the incubator.

For quantitative analysis, three additional T-150 flasks were seeded and allowed to grow until they were approximately 80% confluent. Once confluent, the medium was removed, 10 ml of fresh medium was added to each flask, and the cells were scraped as before. The scraped cells from the three flasks were then combined, and a 10 μl aliquot was removed and counted. Cells (5×10^6) were then added to each of the 15 100-mm^2 tissue culture dishes. The volume of media in the dishes was adjusted to 5 ml with complete growth media. The dishes were then placed in the incubator and allowed to grow for 30 hr.

Kdo$_2$-lipid A preparation

A working solution of Kdo$_2$-lipid A, the active component of bacterial endotoxin (Raetz, 1990), was prepared at a concentration of 100 μg/ml in DPBS. This solution was sonicated for 5 min before each experiment to achieve a uniformly opalescent suspension.

Stimulation and harvesting

RAW 264.7 cells were treated with Kdo$_2$-lipid A to examine the changes in the neutral glyceryl lipids upon activation of the Toll-4 receptor. Cells were stimulated by the addition of 5 μl of the Kdo$_2$-lipid A working solution for a final concentration of 100 ng/ml. They were then incubated for 0.5, 1, 2, 4, 8, 12, and 24 hr. The same volume of DPBS was added to the corresponding control plates. At each time point, a 0.5 ml aliquot of the growth media was removed from each dish and reserved for tumour (TNF-α) analysis. The dishes containing the control and Kdo$_2$-lipid A–treated cells were washed twice with ice-cold DPBS and then scraped into fresh DPBS at a concentration of approximately 16×10^6 cells per ml of buffer. A 50-μl aliquot was reserved for DNA analysis using a fluorescence assay.

Quantitation of DNA

The total amount of DNA in each time course sample was determined using the Quant-iT kit. A standard curve was constructed using the included standards and was linear from 0 to 100 ng. A portion (10 μl) of each reserved sample aliquot and each standard was added to the black 96-well plates. The working solution was prepared as a 1:200 dilution of reagent into the included buffer. An aliquot (190 μl) of this solution was added to each well. Samples were then read on a fluorometer with an excitation wavelength maximum of 510nm and an emission wavelength maximum of 527 nm. The fluorescence of the samples was compared to a calibration curve generated from the fluorescence of the standards to determine the amount of DNA in each sample.

Extraction of total lipids

Total lipids were extracted from the cell suspension. Ice-cold methanol (2.5 ml) was added to each 1 ml of DPBS containing the scraped cell suspension. A volume containing 600 pmol of each of the 18 d$_5$-labeled DAG and TAG internal standards in toluene/methanol (1:1) was added to this suspension for samples being analysed quantitatively. A monophasic solution was formed by the addition of 1.25 ml of CH$_2$Cl$_2$ per ml of cell suspension. This solution was vortexed for 30 s using a benchtop vortex. After the addition of water (1.0 ml) and CH$_2$Cl$_2$ (1.25 ml), the sample was vortexed for an additional 30 s. The phases were then separated by centrifugation at 1000 rpm for 5 min. The lower organic phase was removed to a clean tube using a glass transfer pipette. The upper aqueous phase was reextracted with an additional 2 ml of CH$_2$Cl$_2$. This solution was vortexed and centrifuged as before. The lower organic layer was then combined with that obtained in the first extraction. The total lipid extract was taken to dryness under a gentle stream of nitrogen.

Solid-phase extraction of lipid classes

Total lipids from samples obtained for qualitative analysis were fractionated using Discovery-NH$_2$ solid-phase extraction cartridges following a previously published method. Cartridges containing 500 mg of solid phase were conditioned with 9 ml of hexane. The total lipid extract from 100×10^6 RAW 264.7 cells was loaded in 200 μl of CHCl$_3$. Glyceryl lipids were eluted with 6 ml of CHCl$_3$/IPA (2:1). This fraction was dried under a gentle stream of nitrogen. The samples were dissolved in 1 ml of CHCl$_3$. A 100-μl aliquot of this sample was diluted into 900 μl of CHCl$_3$/MeOH (1:1) to which 20 μl of 0.1 M of NH$_4$OAc was added for a final concentration of 5 mM. These samples were used for qualitative studies.

Glyceryl lipids for quantitative analysis were obtained from the total lipid extract of approximately 8×10^6 RAW 264.7 cells by solid-phase extraction using silica cartridges. Cartridges of 100 mg of material were conditioned with 4 ml of isooctane/ethyl acetate (80:1). The samples were redissolved in 1 ml of isooctane/ethyl acetate (75:25), sonicated for 30 s, and loaded onto the cartridges using a vacuum manifold with the flow-through collected in a clean tube. The neutral lipid fraction was eluted into the same tube with 4 ml of isooctane/ethyl acetate (75:25). This fraction contained the TAGs and DAGs as well as cholesterol and cholesteryl esters, while none esterified fatty acids, monoacylglycerols, and phospholipids were retained on the cartridge. The samples were then taken to dryness under a gentle stream of nitrogen. The samples were dissolved in 200 μl of toluene/methanol (1:1) with 1 mM NH$_4$OAc for MS analysis using an API 4000 Q TRAP (Applied Biosystems, Foster City, CA).

Mass spectrometry

Qualitative analyses were performed on an LTQ, linear ion trap mass spectrometer (Thermo-Finnigan, San Jose, CA). Samples were introduced into the electrospray source using a drawn microcapillary at a flow rate of 1 μl/min. The mass spectrometer was operated in positive ion mode with a spray voltage of 2.4 kV, a capillary temperature of 250°, a capillary voltage of 29.0 V, a 1.5-u ion isolation window, and a 100-ms maximum inject time. Scans (typically 50) were averaged for the MS spectra, and approximately 100 scans were averaged for the MS^2 and MS^3 spectra.

Neutral loss survey experiments were performed on an API 4000 Q TRAP equipped with a NanoMate nano electrospray ionization source (Advion Biosciences, Ithaca, NY). The NanoMate was operated in positive ion mode with a spray voltage of 1.35 kV, vented headspace, and pressure of 0.30 psi, which resulted in a flow rate of approximately 250 nl/min. The mass spectrometer was operated with a step size of 0.10 u, a curtain gas setting of 10, a collision gas setting of medium, a declustering potential of 120, an entrance potential of 10, collision energy of 37, and collision cell exit potential of 6.

The mass-to-charge (m/z) range from m/z 500 to 1200 was scanned over 6 s, giving a total of 30 scans for each neutral loss period. These scans were averaged before submission to the Lipid Profiler software for integration and subsequent analysis. This Applied Biosystems program was modified specifically to process this data format.

Results
Qualitative analysis

Mass spectrometric analysis of the neutral lipid extract from RAW cells yielded a very complex spectrum. From m/z 700 to 1000, peaks corresponded to ammoniated TAG species at nearly every even mass (**Fig. 1**). Each of these m/z values could be assigned a total number of carbon atoms and double bonds based on the mass; however, this designation did not indicate individual molecular species. Multiple isobaric species could exist, differing in the exact individual fatty acyl groups present, positional distribution of fatty acyl groups, double bond location, and geometry. These species could also be straight chained or branched fatty acyl groups. In order to improve the characterization of molecular species to individual fatty acyl groups present (total fatty acyl carbons and total number of double bonds in each fatty acyl group), MS^3 was employed.
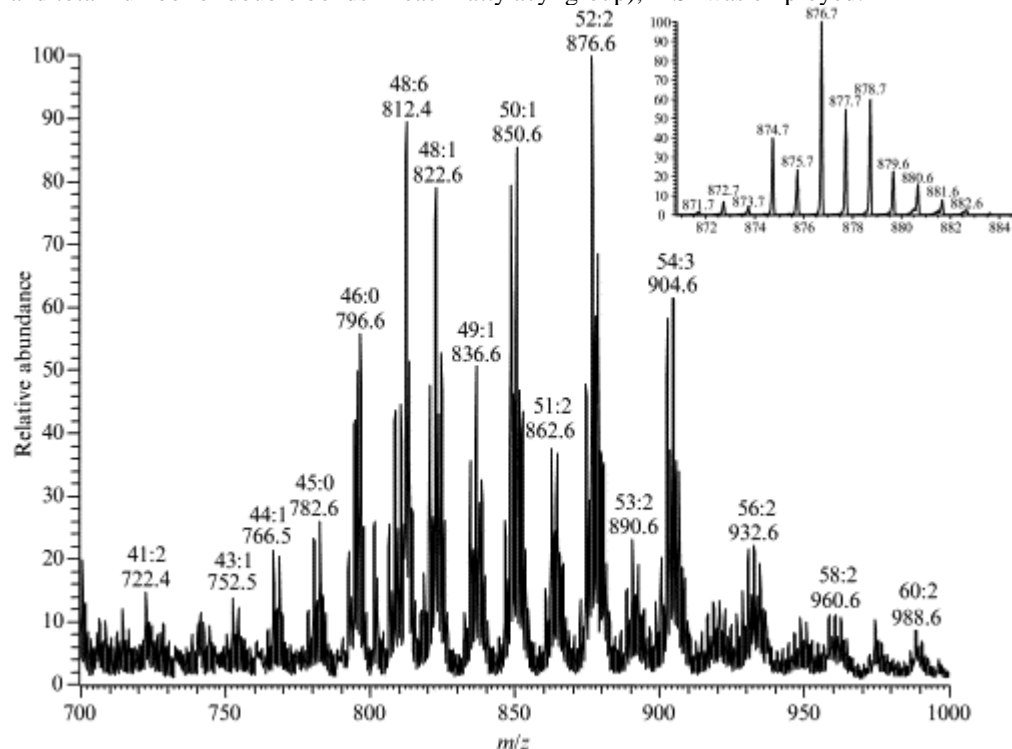

Figure 1. Full-scan mass spectrum of the neutral lipid extract from RAW 264.7 cells showing several envelopes of molecular ions corresponding to triacylglycerols. The envelope corresponding to the series of triacylglycerols containing 52 carbon atoms is shown at high resolution (inset).

For example, the signal at m/z 876 (Fig 1) would correspond to many isobaric combinations of fatty acyl chains with a total of 52 carbons and 2 double bonds or a total of 53 carbons and 9 double bonds within the three esterified

fatty acyl groups. To identify all of the isobaric species present, this strategy used both MS^2 and MS^3 experiments. For the MS^2 case, the TAG [M+NH$_4$]$^+$ parent ion (*m/z* 876) was selected to undergo collision-induced dissociation (CID) (**Fig. 2**). In general, when [M+NH$_4$]$^+$ ions are activated, these ions undergo the neutral loss of a fatty acyl group and ammonia, yielding a corresponding DAG fragment ion. The CID of *m/z* 876 yielded several peaks (*m/z* 549, 575, 577, 603, 605, 619, 631, and 647), each of which corresponded to the loss of a unique fatty acid from one of the isobaric TAG species present at this *m/z* ratio.

The most abundant product ions corresponded to the neutral losses of 18:1 (*m/z* 577), 16:0 (*m/z* 603), and 18:0 (*m/z* 575). The difference in the mass of the [M+NH$_4$]$^+$ precursor ion and the product ion was used to identify the fatty acyl group lost from the total number of carbon atoms and double bonds. The neutral loss masses for several common fatty acyl groups are shown in **Table 1**; however, this neutral loss does not provide information to assign double bond or alkyl branching in the lost fatty acyl group, nor does it indicate to which glycerol carbon atom it was esterified.
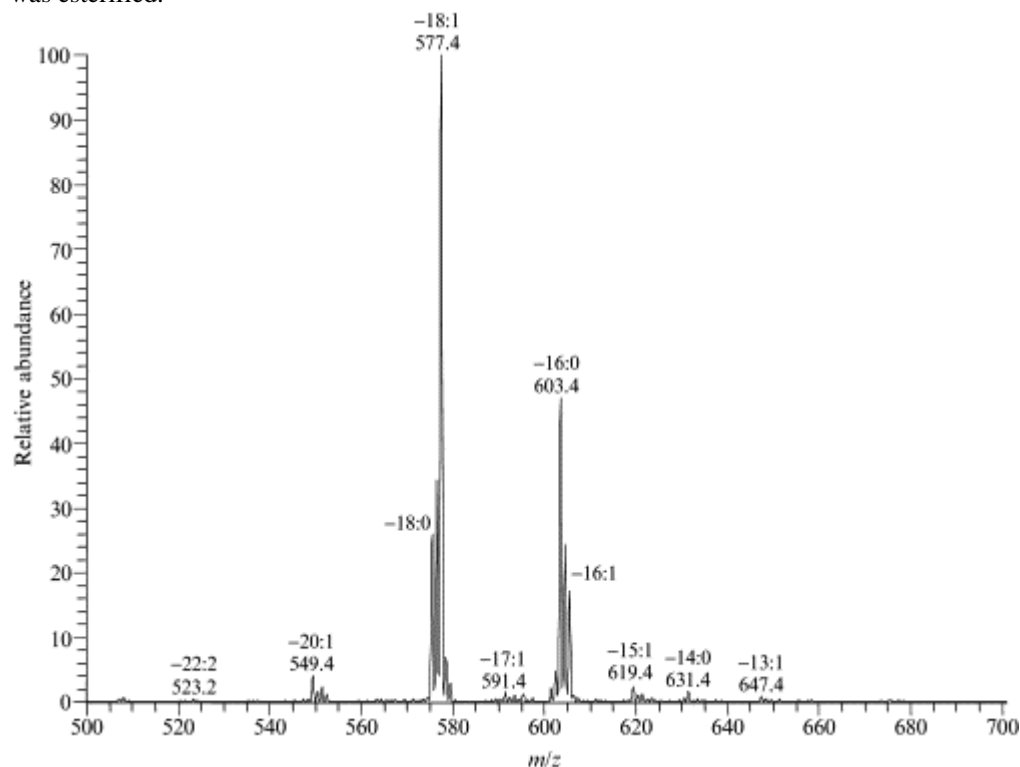

Figure 2. Product ion spectrum from the collision-induced dissociation of the triacylglycerol ion at *m/z* 876 from the full scan at a collision energy of 30 V. The ion at *m/z* 876 undergoes loss of several fatty acyl groups as indicated, with the loss of 16:0 (palmitic acid) and 18:1 (oleic acid) being the most abundant.

Table 1. Neutral loss mass corresponding to common fatty acyl groups esterified to triacylglycerol and diacylglycerol molecular species after collisional activation and observed by tandem mass spectrometry (MS/MS)

Fatty acyl substituent[a]	Neutral loss (u)[b] RCOOH+NH$_3$
14:0[a]	245
15:0	259
16:1	271
16:0	273
17:0	287
18:4	293

Fatty acyl substituent[a]	Neutral loss (u)[b] $RCOOH+NH_3$
18:3	295
18:2	297
18:1	299
18:0	301
19:1	313
19:0	315
20:5	319
20:4	321
20:3	323
20:2	325
20:1	327
20:0	329
21:0	343
22:6	345
22:5	347
22:4	349
22:3	351
22:2	353
22:1	355
22:0	357
24:1	383
24:0	385

[a] Designation of total carbon atoms in the fatty acyl group: total number of double bonds.
[b] Neutral loss in daltons (u) as $RCOOH+NH_3$, which corresponds to the mass of the fatty acyl group as a free carboxylic acid plus the mass of ammonia.

From the MS^2 spectrum, a product ion can be selected for further fragmentation in the linear ion trap. Collision-induced dissociation of the DAG product ions yielded information about both remaining fatty acyl substituents. The mass of the MS^3 product ions related directly to the final esterified acyl chain, and the difference in mass between the MS^2 precursor and MS^3 product ion gave information about the fatty acyl chain that was lost as a neutral species. As shown for the initial MS^2 product ion at m/z 577 (**Fig. 3**), collision-induced dissociation led to a number of MS^3 product ions corresponding to the remaining fatty acyl chains as acylium ions ($[RCO]^+$) and as fatty acids esterified to the glycerol backbone ($[R'+74]^+$) with their associated losses of water. For example, the presence of an 18:1 fatty acyl component in the MS^2 product ion m/z 577 was revealed by the abundant MS^3 product ion at m/z 265 that corresponds to $C_{17}H_{33}C=O^+$, while the presence of 16:0 was revealed by the MS^3 product ion at m/z 239 ($C_{15}H_{31}C=O^+$) and 313 ($[C_{15}H_{31}COO-CH_2CH_2CHO] + H^+$). The mechanism for the formation of these ions had been described previously from labelling studies in which the hydrogen atoms on the glycerol backbone were replaced with deuterium atoms.
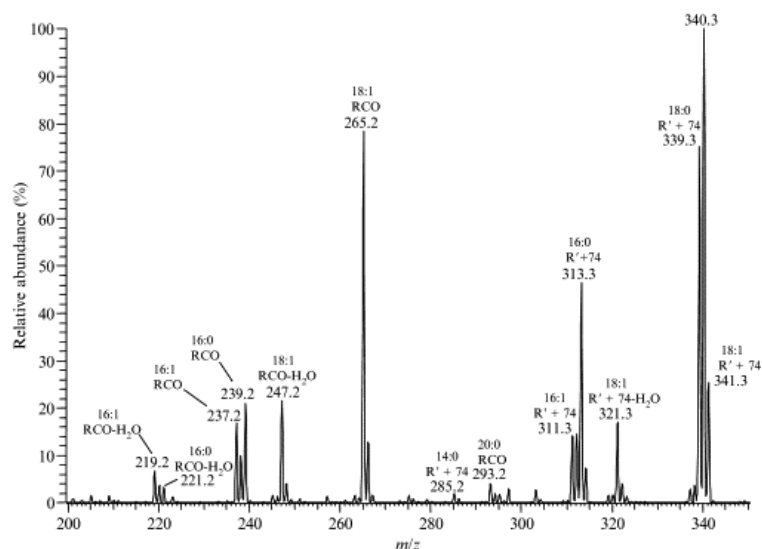
Figure 3. MS/MS/MS spectrum of the diacyl product ion at *m/z* 577 resulting from the collision-induced dissociation of the ion at *m/z* 876 in the mass spectrum. The ion at *m/z* 577 was selected in the linear ion trap to undergo collision-induced dissociation to determine the nature of the final fatty acyl species present in the isobaric molecules. Both acylium ions ([RCO]$^+$) and ions retaining the glycerol backbone ([R'+74]$^+$) are present in this spectrum.

From the information obtained from the MS^2 and MS^3 spectra, a table containing all the isobaric species identified for a specific *m/z* value was generated. As shown in Table 2, for the three most abundant fragment ions observed in the MS^2 spectrum of the ion at *m/z* 876 (*m/z* 577, 603, and 575), the DAG ions, subjected to MS^3, yielded product ions with unique structural information. From a single [M+NH$_4$]$^+$ ion, the identity of approximately 100 distinct molecular species (not counting stereoisomers and double-bond isomers) could be determined. Some species such as 16:0/18:1/18:1 or 16:0/18:0/18:2 would be predicted by the total carbons and double bonds present in the species and the relatively common nature of the fatty acids; however, the presence of these molecular species is directly supported by product ions from several MS^3 spectra. Other species were seen that would not be expected without mass spectral evidence. These included 17:1/18:1/17:0, which was observed in the MS^3 spectra of *m/z* 577 (loss of 18:1) and 591 (loss of 17:1), and 16:1/14:0/22:1, which was observed in the MS^3 spectra of *m/z* 605 (loss of 16:1) and 631 (loss of 14:0). Each of the molecular species in Table 2 was confirmed by ions in multiple spectra. Some species were repeated in Table 2 because their presence was suggested by ions in more than one MS^3 spectrum; however, species corresponding to 53:9 could not be found.

Quantitative analysis

A quantitative method for accurate determination of changes in molecular species components in the complex mixture of neutral lipids containing a number of isobaric species was developed utilizing the characteristic fragmentation pathways. Deuterium-labelled internal standards, whose masses fell into regions of the spectrum that did not contain ions corresponding to ammoniated DAG and TAG molecular species, afforded a means for normalization of neutral loss data for 18 different fatty acyl groups.

Neutral loss experiments were performed to follow changes in Kdo$_2$-lipid A–treated cells in terms of DAG and TAG molecular species that contained at least one of the 18 different fatty acyl groups present in the deuterium-labelled internal standards. Each neutral loss corresponding to one of the 18 fatty acyl groups in the deuterated internal standards (**Table 3**) was monitored for a period of 3 min, yielding a characteristic total ion current (**Fig. 4**). For each period in the experiment, a unique neutral loss spectrum was obtained, which revealed all of the [M+NH$_4$]$^+$ ions in the complex mixture that contained a single fatty acyl group as well as some indication of the abundance of this [M+NH$_4$]$^+$ ion relative to a deuterium-labelled internal standard (**Fig. 5**). For example, the presence of 18:1 esterified to DAG molecular species gave abundant ions at *m/z* 612, 638, and 668. The ion at *m/z* 612 would correspond to an 18:1/16:0 DAG, *m/z* 638 an 18:1/18:1 DAG, and *m/z* 668 an 18:1/20:0 DAG molecular species (Fig. 5A). The abundance of these molecular species compared to the internal standard at *m/z* 827.8 was monitored in a series of experiments covering the course of Kdo$_2$-lipid A stimulation, revealing changes in each DAG species taking place. However, it would not be possible to state relative abundance of 18:1/18:1 DAG and 18:1/16:0 DAG to each other because of the difference in neutral loss behaviour due to structural features such as esterification position on the glycerol backbone. Each neutral loss experiment revealed

common and new molecular species, such as species containing 16:0 (**Fig. 5B**) and 16:1 (**Fig. 5C**). Thus, these spectra gave unique identification of DAG species, but only partial characterization of TAG species.

Table 2. Triacylglycerol molecular species identified from the MS/MS/MS (MS^3) analysis of the three most abundant diacylglycerol product ions observed in the tandem mass spectrometry (MS/MS) (MS^2) spectrum of the $[M+NH4]^+$ triacyglycerol observed at m/z876 in the full mass spectrum of RAW 264.7 cells

MS^2product ion[a]	Triacylglycerol[b]	MS^3ion type	MS^2product ion[a]	Triacylglycerol[b]	MS^3ion type	MS^2product ion[a]	Triacylglycerol[b]	MS^3ion type
577 (−18:1)	18:1/18:1/16:0	RCO	603 (−16:0)	16:0/18:1/18:1	RCO	575 (−18:0)	18:0/18:1/16:1	R'+74
	18:1/14:1/20:0	R'+74-H_2O		16:0/14:1/22:1	R'+74- H_2O		18:0/18:1/16:1	RCO
	18:1/18:1/16:0	R'+74		16:0/18:1/18:1	R'+74		18:0/14:1/20:1	R'+74- H_2O
	18:1/18:0/16:1	R'+74		16:0/18:1/18:1	RCO- H_2O		18:0/16:1/18:1	R'+74
	18:1/18:1/16:0	RCO- H_2O		16:0/18:1/18:1	R'+74- H_2O		18:0/16:1/18:1	RCO
	18:1/16:0/18:1	RCO		16:0/20:1/16:1	R'+74		18:0/12:1/22:1	R'+74- H_2O
	18:1/12:0/22:1	R'+74- H_2O		16:0/16:0/20:2	R'+74		18:0/16:0/18:2	R'+74
	18:1/22:1/12:0	RCO		16:0/18:2/18:0	R'+74- H_2O		18:0/16:1/18:1	RCO- H_2O
	18:1/17:3/18:5	R'+74		16:0/18:0/18:2	R'+74		18:0/18:1/16:1	RCO- H_2O
	18:1/18:1/16:0	R'+74- H_2O		16:0/18:2/18:0	R'+74		18:0/18:1/16:1	R'+74- H_2O
	18:1/16:1/18:0	RCO		16:0/19:0/17:2	R'+74- H_2O		18:0/22:1/12:1	RCO
	18:1/12:1/22:0	R'+74- H_2O		16:0/17:2/19:0	R'+74		18:0/18:2/16:0	R'+74
	18:1/16:1/18:0	R'+74		16:0/18:0/18:2	R'+74- H_2O		18:0/19:0/15:2	R'+74- H_2O
	18:1/16:1/18:0	RCO- H_2O		16:0/20:2/16:0	R'+74- H_2O		18:0/20:1/14:1	RCO
	18:1/20:1/14:0	RCO		16:0/18:2/18:0	RCO		18:0/16:1/18:1	R'+74- H_2O
	18:1/16:1/18:0	R'+74- H_2O		16:0/19:0/17:2	RCO- H_2O		18:0/18:2/16:0	R'+74- H_2O
	18:1/19:0/15:1	R'+74- H_2O		16:0/18:2/18:0	RCO- H_2O		18:0/22:2/12:0	RCO
	18:1/22:1/12:0	RCO- H_2O		16:0/20:1/16:1	RCO		18:0/18:2/16:0	RCO- H_2O
	18:1/16:0/18:1	RCO- H_2O		16:0/16:1/20:1	R'+74- H_2O		18:0/18:2/16:0	RCO
	18:1/15:1/19:0	R'+74		16:0/20:2/16:0	R'+74		18:0/19:0/15:2	RCO- H_2O
	18:1/14:0/20:1	R'+74		16:0/21:0/15:2	R'+74- H_2O		18:0/14:2/20:0	R'+74- H_2O
	18:1/18:0/16:1	RCO		16:0/20:2/16:0	RCO		18:0/14:0/20:2	R'+74
	18:1/14:0/20:1	R'+74- H_2O		16:0/21:0/15:2	RCO- H_2O		18:0/22:1/12:1	RCO- H_2O
	18:1/20:0/14:1	RCO		16:0/16:2/20:0	R'+74- H_2O			
	18:1/16:0/18:1	R'+74- H_2O		16:0/16:1/20:1	RCO			
	18:1/22:0/12:1	RCO		16:0/16:1/20:1	R'+74			
	18:1/18:0/16:1	R'+74- H_2O		16:0/20:2/16:0	RCO- H_2O			
	18:1/23:0/11:1	RCO- H_2O		16:0/14:0/22:2	R'+74			
	18:1/15:1/19:0	RCO- H_2O		16:0/15:1/21:1	RCO- H_2O			
	18:1/20:1/14:0	RCO- H_2O		16:0/20:1/16:1	RCO- H_2O			
	18:1/19:0/15:1	RCO- H_2O		16:0/16:1/20:1	RCO- H_2O			
	18:1/14:1/20:0	RCO		16:0/15:1/21:1	RCO			
	18:1/15:1/19:0	RCO		16:0/20:1/16:1	R'+74- H_2O			
	18:1/12:0/22:1	R'+74		16:0/21:1/15:1	RCO- H_2O			
	18:1/13:1/21:0	RCO		16:0/19:1/17:1	RCO			
	18:1/17:1/17:0	RCO		16:0/15:1/21:1	R'+74- H_2O			
	18:1/15:1/19:0	R'+74- H_2O		16:0/13:0/23:2	R'+74			
	18:1/14:0/20:1	RCO- H_2O		16:0/17:1/19:1	RCO			
	18:1/18:0/16:1	RCO- H_2O						

a   The neutral loss from m/z 876 to the MS^2 product ion revealed one of the fatty acyl groups in this $[M+NH_4]^+$ species in parentheses under the mass of the MS^2 product ion.

b   Each TAG column has the first entry in the TAG molecular species abbreviation, by default, as the species that was lost as a neutral in MS^2. The second entry in the abbreviation is the acyl group indicated by the presence of the specified ion type in the MS^3 spectrum (column 3) and the third entry of the abbreviation was calculated from the mass difference of the two.

Table 3. [1,1,2,3,3-d5] Glycerol-labelled glyceryl lipids used as internal standards for neutral loss mass spectrometric analysis

| Triacylglycerol fatty acyl composition	m/z $[M+NH_4]^+$	Diacylglycerol fatty acyl composition	m/z $[M+NH_4]^+$
19:0/12:0/19:0a	857.83	19:0/19:0	675.66
14:0/16:1/14:0	771.73	20:0/20:0	703.7
15:0/18:1/15:0	771.73	14:0/14:0	535.51
16:0/18:0/16:0	857.83	15:0/15:0	563.54
17:0/17:1/17:0	869.83	16:0/16:0	591.57
20:4/18:2/20:4	949.8	17:0/17:0	619.57
20:0/20:1/20:0	995.97	20:2/20:2	695.6
20:2/18:3/20:2	955.84	20:4/20:4	687.54
20:5/22:6/20:5	993.77	20:5/20:5	683.51

a The acyl order as indicated: sn-1/sn-2/sn-3.
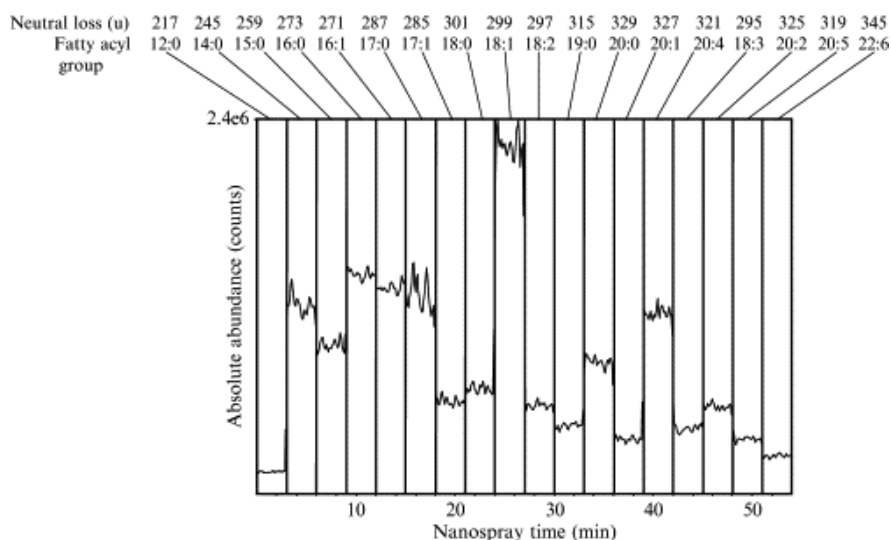
Figure 4. Total ion current from a neutral loss survey in the time course of glyceryl lipid changes upon activation of the Toll-4 receptor in RAW 264.7 cells. Each column represents a 3-min period in which the neutral loss of a different fatty acyl moiety from the diacylglycerol and triacylglycerol species was monitored.

The Lipid Profiler software package was used to integrate the ion abundance for each m/z, to correct abundances due to ^{13}C isotopes, and to identify DAG and TAG ions and the internal standards in the averaged spectra from each period in the neutral loss survey. The corrected DAG and TAG abundances were normalized to the abundance of the internal standards.

Changes in the abundance of specific species compared to the internal standard over time in the control and Kdo2-lipid A–treated cells were thereby assessed in a quantitative way (**Fig. 6**). This quantitative approach revealed time-dependent changes in the 14:0/16:0 DAG molecular species in Kdo2-lipid A–treated RAW cells, as measured by the neutral loss of 14:0 (**Fig. 6A**) or 16:0 (**Fig. 6B**). The abundance of 14:0/16:0 DAG in Kdo2-lipid A–treated cells was greater than that in control samples, with very similar time dependence, regardless of which neutral loss was monitored.

The neutral loss of 16:1 was common to several TAG molecular species; however, in some cases, a significant increase was observed between the ratios of abundances for molecular species in treated and control samples at 24 hr, as is the case for the 48:1 TAG molecular species that contain 16:1 (**Fig. 7A**). For the 48:3 TAG containing 16:1 (**Fig. 7B**), though, the relative abundance was constant for treated cells compared to controls at 24 h.

The analysis of glyceryl lipids present within mammalian cells is very challenging. However, the power of combining MS^2 and MS^3 can be used to uniquely identify TAGs and DAGs and to quantitate molecular species with a specific total of fatty acyl carbon atoms and double bonds and containing a specific fatty acyl group from a very complex biological sample in the neutral lipid extract of RAW 264.7 macrophages. This approach can be used to precisely assess changes within populations of molecular species that cannot be determined by measurement of molecular ion species such as $[M+H]^+$, $[M+Li]^+$, or $[M+NH_4]^+$ abundances alone. However, these stable isotope-controlled MS^2 and MS^3 experiments do not provide molar concentration data and, in the case of TAG molecules, do not analyse the complex mixture to the extent of providing molecular species information, stereochemistry, or even positional analysis.
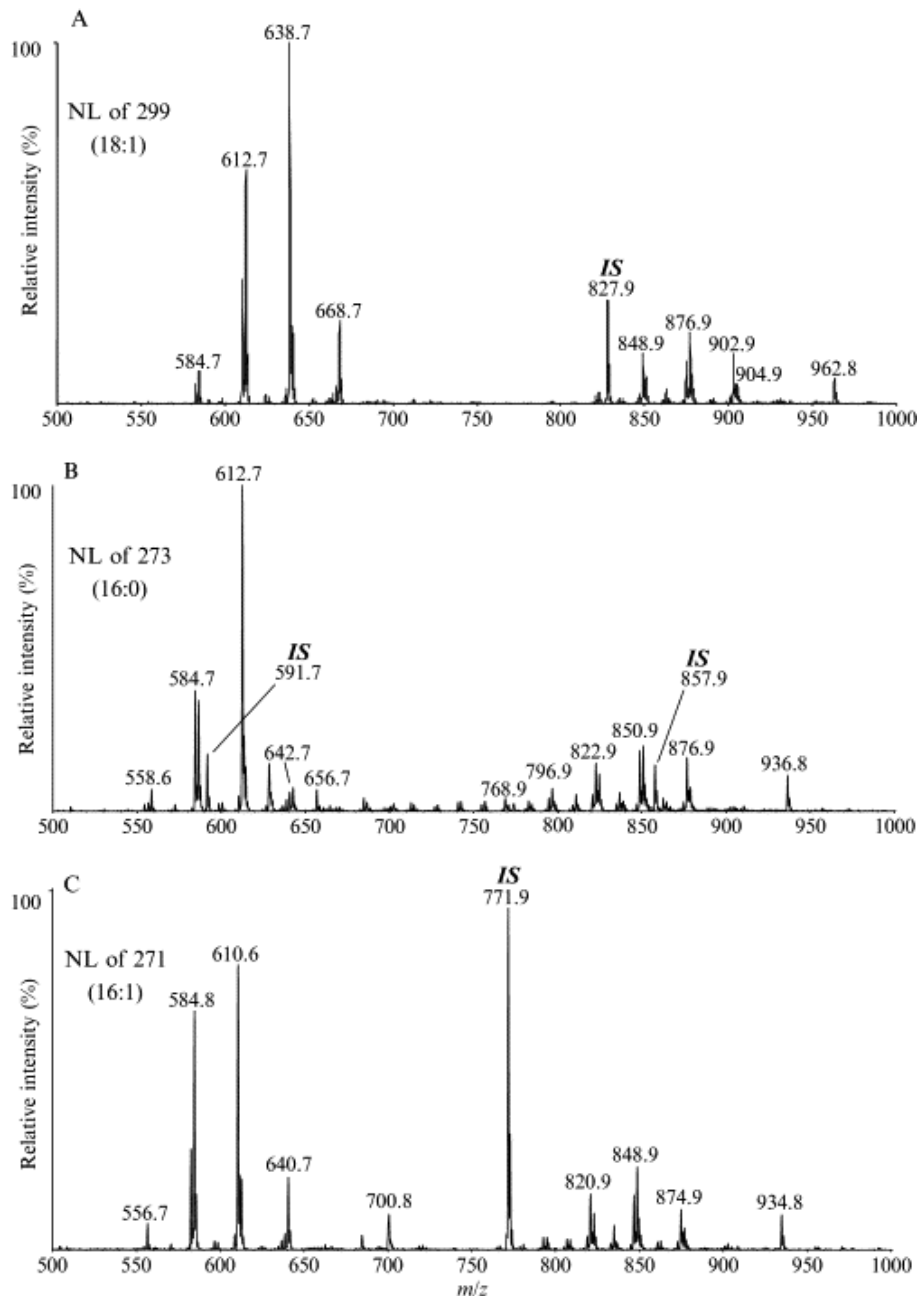

Figure 5. Spectra showing the $[M+NH_4]^+$ ions detected by the neutral loss of an 18:1, 16:0 or 16:1 fatty acyl group upon collisional activation. In this case, the diacylglycerolspecies can be uniquely identified, but the triacylglycerol molecular species can only be partially elucidated.
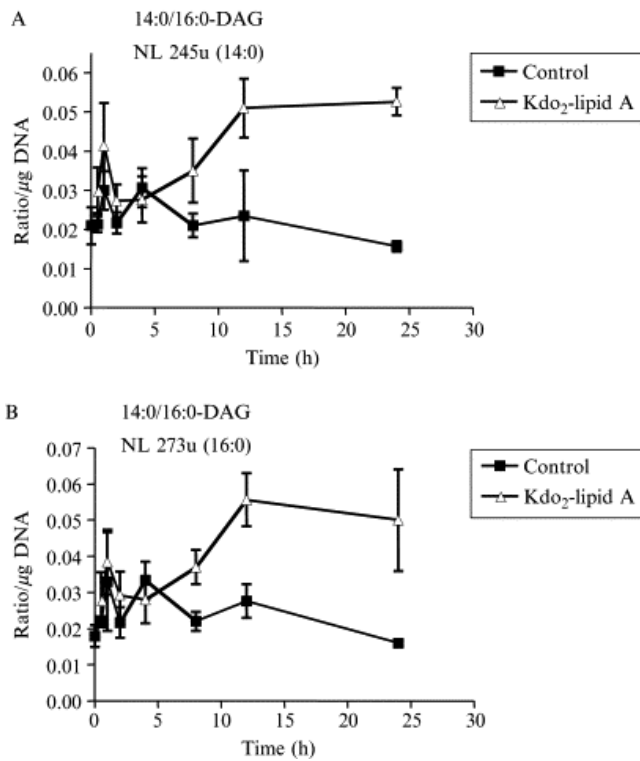
Figure 6. (A) Quantitative analysis showing the increase in abundance of the 14:0/16:0 diacylglycerol over time in Kdo_2-lipid A–treated cells compared to control measured from the neutral loss of 14:0. (B) Quantitative analysis showing the increase in abundance of the 14:0/16:0 diacylglycerol over time in Kdo_2-lipid A–treated cells compared to control measured from the neutral loss of 16:0.
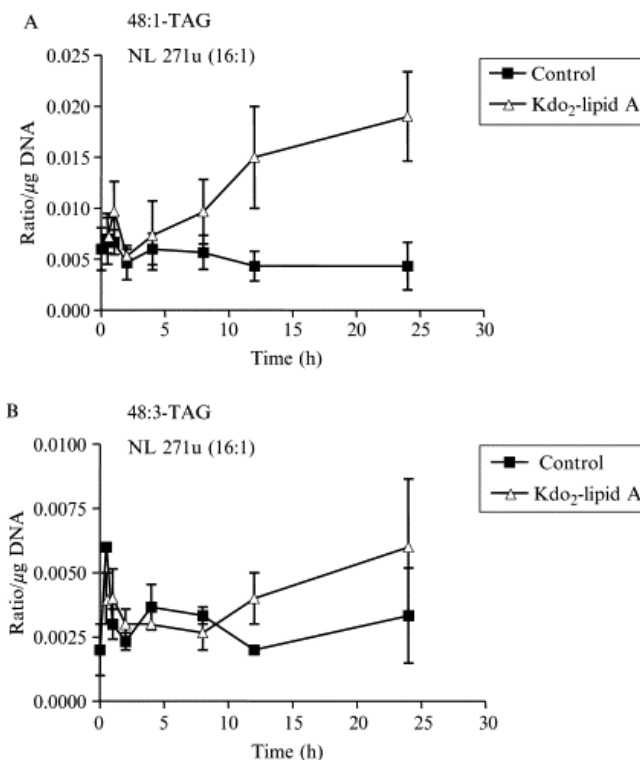

Figure 7. (A) Quantitative analysis of the changes in the 48:1 triacylglycerol molecular species which contains a 16:1 fatty acyl group. The abundance of this species changes in Kdo_2-lipid A–treated cells compared to controls. (B) Quantitative analysis of the changes in the 48:3 triacylglycerol molecular species that contains a 16:1 fatty acyl group. The abundance of this species in Kdo_2-lipid A–treated cells does not change compared to control.